Solid State Ionics 337 (2019) 147–153

Contents lists available at ScienceDirect

Solid State Ionics

journal homepage: www.elsevier.com/locate/ssi

Preparation and characterization of a new ternary PVA-based electrolyte for "all solid state" Zn/MnO_2 cell

Zahia Gharnout[a,b,*], Laid Telli[b], Abdallah Merrouche[b], Larbi Zerroual[c], Serge Walter[d]

[a] Département de SNV, Institut des Sciences et de la Technologie, Centre Universitaire Abdelhafid Boussof-Mila, 43000, Mila, Algeria
[b] Laboratoire des Matériaux Inorganiques, Faculté des Sciences, Université Mohamed Boudiaf-M'sila, 166, rue d'Ichbilia, 28000 M'sila, Algeria
[c] Laboratoire de Génie des Procédés Chimiques (LGPC), Faculté de Technologie, Université Ferhat Abbas Sétif-1, 19000 Sétif, Algeria
[d] Laboratoire Propre Intégré (LPI), Groupe Sécurité et Ecologie Chimiques (GSEC), ENSCMu, 3 rue Alfred Werner, F-68093 Mulhouse Cedex, France

ARTICLE INFO

Keywords:
Solid polymer electrolyte
PVA
Ethylene glycol
Plasticizer
Protonic conductivity
Impedance spectroscopy

ABSTRACT

A solid polymer electrolyte with a polyvinyl alcohol (PVA) matrix and a mixture of ethylene glycol (EG) and phosphoric acid as proton conductor has been developed. These complexes have been studied by X-ray diffraction (XRD), infrared Fourier transform spectrometry (FTIR) and electrochemical impedance spectrometry (EIS). The optimum ionic conductivity value of the ternary PVA-EG(45 wt%)-H_3PO_4(5 wt%) complex film has been achieved to be $5.2\ 10^{-3}$ S cm^{-1} at RH = 100% with adequate mechanical properties (especially flexibility) and with a low activation energy of 9 kJ mol^{-1}. Due to its good electrical and mechanical properties, this material has been successfully used as solid state proton electrolyte in Zn/MnO_2 cell delivering a capacity of 220 Ah kg^{-1} and an energy density of up to 286 Wh kg^{-1}.

1. Introduction

The demand of electrical energy is growing in the world especially for powering portable or nomadic devices such as portable microcomputers, mobile phones, electrical vehicles … etc. In this area, the development of existing electrochemical batteries and the research of new systems become an absolute necessity. However, batteries with liquid electrolytes have many advantages and find since a long time a real success. Nonetheless, these batteries suffer from several drawbacks mainly related to the physical state of the electrolyte. In order to overcome these drawbacks, many efforts have been directed towards the substitution of liquid electrolytes with solid ionic conductors. Indeed, the use of all-solid state batteries solves most of the problems observed in conventional liquid electrolyte systems. In these systems, the electrode active materials should accept charging and discharging, respectively, insertion and extraction of low ionic radius mobile ions in the electrolyte such as H^+, Li^+, Ag^+ etc. However, most contributions in this area have been made with lithium batteries because of the availability of good Li^+ solid conductors, wide electrochemical stability window [1,2] and high energy density batteries [3]. Nonetheless, lithium-ion batteries suffer from serious drawbacks related to reactivity of lithium and their excessive cost [4]. To overcome these limitations, new all-solid state batteries of low cost and perfect safety have been developed.

Since the ionic radius of H^+ is lower than that of Li^+, all-solid protonic batteries can constitute an alternative of lithium batteries. Despite their low electrochemical stability window, compared with that of lithium batteries, these all-solid protonic batteries are perfectly suitable for applications requiring low power density.

In recent years, solid polymer electrolytes (SPE) have attracted considerable attention owing to their numerous potential applications in electrochemical devices particularly in solid state batteries, sensors, fuel cells and supercapacitors [5–8]. Indeed, these solid polymer electrolytes have several desirable advantages compared with liquid electrolytes. For instance, possibility of forming thin films of suitable sizes, good mechanical properties in particular flexibility, possibility of miniaturization and ability to form appropriate electrode/electrolyte contacts [9–11]. Nevertheless, they have a relatively low ionic conductivity at room temperature, which limits their use in the grand-public batteries.

To improve the ionic conductivity of such materials, complexes formed of a polymeric matrix and a mineral load have been developed. Among the polymeric matrixes, the PVA, beside the polyethylene oxide (PEO), finds a place of choice in this domain when it is associated with potassium hydroxide (KOH) [12–15], orthophosphoric acid [16–19] or phosphotungstic acid (PWA) [20–26]. Indeed, ternary complexes PVA-SiWA-PWA, PVA-SiWA-H_3PO_4 and PVA-PWA-H_3PO_4, have a sufficiently high ionic conductivity that reaches 10^{-2} S cm^{-1} [11,27,28]

* Corresponding author at: Département de SNV, Institut des Sciences et de la Technologie, Centre Universitaire Abdelhafid Boussof-Mila, 43000, Mila, Algeria.
E-mail address: gharnoutzahia@yahoo.fr (Z. Gharnout).

https://doi.org/10.1016/j.ssi.2019.04.012
Received 9 April 2019; Accepted 15 April 2019

and mechanical properties appropriate to their use as a solid electrolyte in batteries. However, the presence of an important amount of acid associated to PVA in these complexes engenders the corrosion of the negative electrode of the cell. To minimize this corrosion and maintain the cell at its high performances, we propose a total or partial substitution, of the acid by a neutral additive. Knowing that the ionic conductivity of such materials depends on the concentration of mobile charge carriers (H^+) and their mobility [29–31], the association to PVA a plasticizer such as ethylene glycol may lead to form an amorphous complex and consequently ensures a sufficiently high electrical mobility of the ions. However, if the contribution of the plasticizer in the enhancement of the electrical conductivity is insufficient, the addition of a low amount of H_3PO_4 to PVA-based complexes may be envisaged. The composition of these new complexes should be optimized to satisfy their use in "all-solid" Zn/MnO_2 cells.

2. Experimental

2.1. Materials

PVA-based complexes have been prepared according to the same procedure described in our previous work [28]: 1 g of PVA (polyvinyl alcohol, with an average molecular weight of about 7 10^4 g mol^{-1}, MERCK) is dissolved in 100 cm^3 of boiling water under vigorous stirring until complete dissolution of the polymer. Once PVA is completely dissolved, an appropriate amount of ethylene glycol (EG: HO-CH_2-CH_2-OH, molecular weight 62.07 g mol^{-1}, BIOCHEM, wt% EG: 0–50 wt%) and H_3PO_4 (85% phosphoric acid, PROLABO: 0–10 wt%) are added to the previous solution. The mixture is then heated at 80 °C until obtaining a highly viscous gel with a remaining liquid around 20% of its initial volume. The gel obtained is poured on a flat smooth surface of a cylindrical PETRI glass box to obtain, after drying in ambient atmosphere for a few days, homogeneous films having comparable thicknesses (with an average of 0.20 ± 0.005 mm). The films thus obtained were cut to form circular samples of 13 mm in diameter and stored under appropriate conditions before testing.

2.2. XRD and FTIR studies

The characterization of the different samples has been made by means of a high resolution MRD PANALYTICAL (ISM) X-Ray diffractometer using Cu K_α radiation with a wavelength of 0.15418 nm for 2θ varying between 5 and 70° and stepping by 0.01° s^{-1}.

The FTIR measurements have been recorded using a SHIMADZU 8400S FTIR spectrometer in the spectral range 4000 to 400 cm^{-1} with resolution of 2 cm^{-1}.

2.3. Electrical and electrochemical characterization

The ionic conductivity measurements were realized by conducted with a Solartron 1260 type impedance-meter controlled by computer using Zplot and Zview software. For these measurements, the frequency range was 1 to 10^6 Hz and the ac applied voltage was 10 (for the highest conductivities) to 50 mV (for less conductive materials). While, for the electrochemical characterization of the studied systems the frequency range used extends from 10 mHz to 1 MHz with an ac applied voltage of 10 mV.

2.4. Cell assembly

The prepared PVA-based complexes, that present appropriate mechanical and electrical properties, were used as solid electrolyte of Zn/MnO_2 cells. These cells have been realized according to the same procedure described earlier [28]. The active masses of the electrodes of the cell were prepared separately, assembled with the electrolyte previously prepared and stored under controlled atmosphere. An appropriate amount (80 mg) consisting of a homogenized mixture of a manganese dioxide powder (variety γ, Sedima) and carbon black (CB: with a percentage range from 0 to 5 wt%) was pressed to form a pellet (diameter = 13 mm and thickness = 0.01 mm) using a hydraulic press (800 MPa cm^{-2}). Following the same steps described previously, a pellet of the negative active mass (40 mg) was prepared from a mixture of metallic Zn (Prolabo), hydrated salt zinc (zinc ammonium sulfate, noted AZS with a chemical formula: $(NH_4)_2Zn(SO_4)_2.6H_2O$) previously prepared in the laboratory and carbon black [32]. The composition of the negative active mass corresponds to a weight ratio (wt%) zinc: hydrated salt zinc: carbon black equal to 65:(35-x):x where x varies from 0 to 5. This mixture is carefully homogenized using an agate mortar. The cells destined for the electrochemical study, were assembled according to the following order: positive active mass, electrolyte, negative active mass. The battery is covered with a flexible 0.25 mm graphite foil on each side. The all solid system is then placed between two stainless steel current collectors and kept under moderate pressure using a Teflon screwing system. For specific studies, the cells were prepared in the same manner as described previously expect that the Zn-based pellet is divided into two equal and symmetrical parts, one of which forms the working electrode and the other is used as a reference electrode [33]. To control the hydration of the different materials used, all the electrical and electrochemical measurements of the above described systems were carried out under controlled relative humidity and fixed temperature.

3. Results and discussion

3.1. X-ray diffraction

Fig. 1 shows the x-ray diffractograms of pure PVA, PVA-EG(50 wt %), PVA-H_3PO_4(5 wt%) and PVA-EG(45 wt%)-H_3PO_4(5 wt%) complexes. The PVA film diffraction pattern (Fig. 1a) presents a broad peak at 2θ = 20° characteristic of an amorphous structure of the polymer [26,34–36]. Similar diffraction patterns of PVA-EG(50 wt%) (Fig. 1b), PVA-H_3PO_4(5 wt%) (Fig. 1c) and PVA-EG(45 wt%)-H_3PO_4(5 wt%) (Fig. 1d) complexes to that of PVA were obtained. Nevertheless, the intensity of the characteristic ray of the polymeric phase becomes weaker with the addition of the plasticizer and/or H_3PO_4. This shows the plasticizing effect of ethylene glycol and phosphoric acid in the complex. On the other hand, the substitution of 5 wt% of ethylene glycol by an equivalent quantity of orthophosphoric acid engenders a more important effect on the intensity and the width of the characteristic ray of the polymer. It shows clearly that the amorphous character of the studied complexes becomes more pronounced with the addition of EG and H_3PO_4. Similar results were published in the literature [16,37–39].

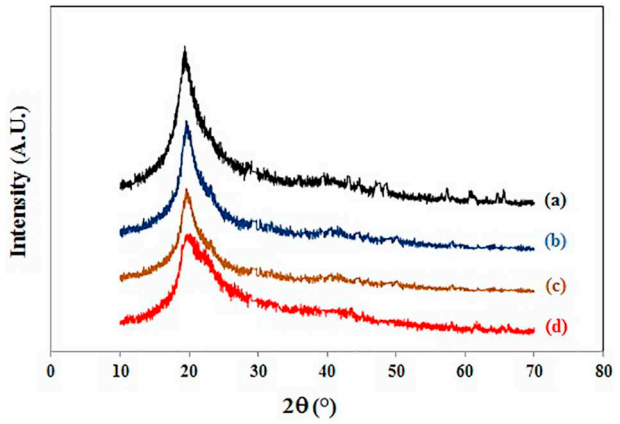

Fig. 1. X-ray diffraction patterns of: (a) PVA, (b) PVA-EG(50 wt%), (c) PVA-H_3PO_4(5 wt%) and (d) PVA-EG(45 wt%)-H_3PO_4(5 wt%).

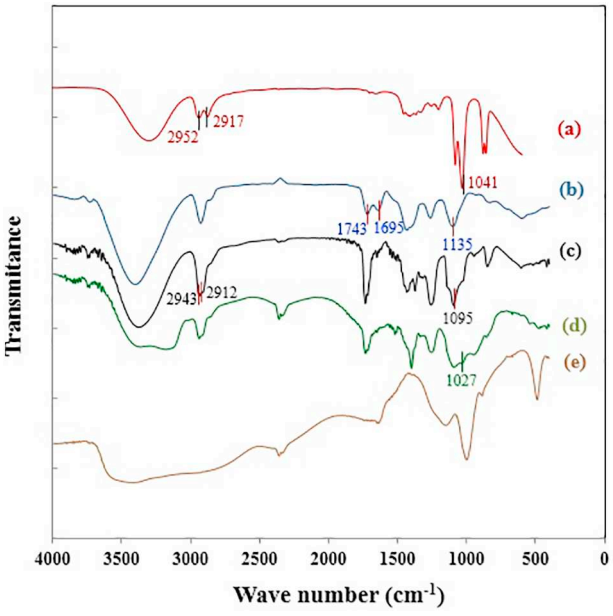

Fig. 2. FTIR spectra of: (a) EG, (b) PVA-EG(30 wt%), (c) PVA, (d) PVA-H_3PO_4(30 wt%) and (e) H_3PO_4.

3.2. Fourier transform infrared spectrometry (FTIR)

Fig. 2 illustrates the infrared spectra of binary PVA-EG(30 wt%) and PVA-H_3PO_4(30 wt%) complexes in comparison with the pure initial compounds: PVA, EG and H_3PO_4. On the IR spectrum of the PVA (curve c) appears four peaks at 3467 2943, 2912 and 1095 cm^{-1} attributed to the vibration of O—H, CH_2, C—H and C—OH groups respectively [16,20,40]. Thus, the infrared spectrum of ethylene glycol (curve a) shows the presence of four bands located at 3353, 2952, 2917 and 1041 cm^{-1}, that correspond respectively to the vibration of O—H, CH_2, CH and C—OH [41–43]. However, on the IR spectrum of the PVA-EG(30 wt%) complex (curve b) the band related to C—OH, which appeared at 1095 cm^{-1} and 1041 cm^{-1} on the spectra of the PVA and EG respectively, becomes larger with a slight shift towards the higher values of the wave number (1135 cm^{-1}). This demonstrates the interaction between the molecules of ethylene glycol and the OH groups of PVA. This last band is the consequence of the formation of the C—O—C link in the complex [16,39,41]. In addition, we note the presence of two bands located at 1695 and 1743 cm^{-1} corresponding to the vibration of C═O groups of residual acetate [16,19,44,45] used as precursor of the PVA.

On the IR spectrum of the PVA-H_3PO_4(30 wt%) complex (curve d), a double band appears in the region 3200–3500 cm^{-1}, showing the presence of two types of OH bands. The first one related to the vibration of the OH group of the polyvinyl alcohol [16,20,28,46,47] and the second corresponds to the vibration of the OH group of orthophosphoric acid. However, the band at 1027 cm^{-1} that corresponds to the vibration of C-O-P [28,48–50] proves that at last some of the OH groups of PVA have been transformed by the phosphoric acid.

3.3. Hygrometry

The behaviour of the various PVA-EG complexes has been studied as a function of the surrounding relative humidity. The hydration of these complexes has been determined at equilibrium by gravimetry. The values of the evolution of the mass measured have been referred to a same standard sample mass. Some typical results of the evolution of the mass of the studied complexes as a function of RH are shown in Fig. 3.

The studied binary complexes PVA-EG form flexible films and remain in the solid state for all ethylene glycol rate used and all the explored relative humidity range (10 to 100%). They show a hygrometric behaviour similar to that of the previously studied complexes [28].

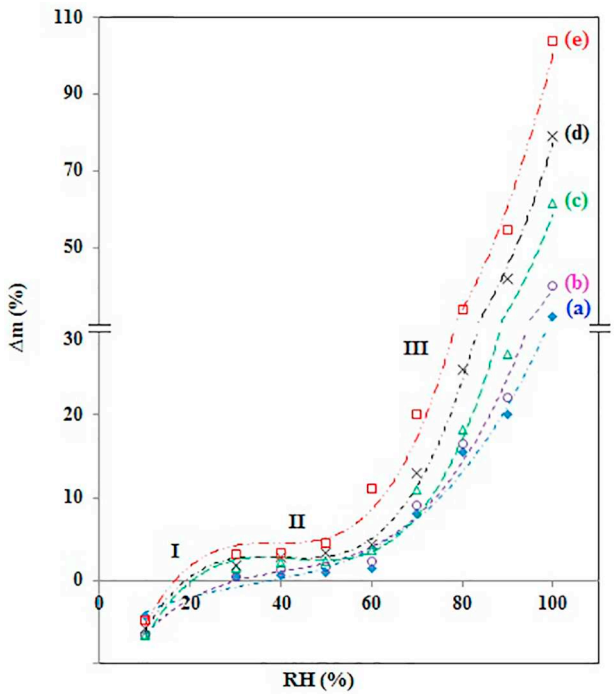

Fig. 3. Sample weight variation Δm (%) as a function of relative humidity at 25 °C of: (a) PVA, (b) PVA-EG(10 wt%), (c) PVA-EG(30 wt%), (d) PVA-EG(50 wt%) and (e) PVA-EG(45 wt%)-H_3PO_4(5 wt%).

PVA-EG complexes and PVA show a hygrometric behaviour practically stable and comparable between 10 and 70% RH (region I and II in Fig. 3). In region II, the mass of these complexes remains practically constant. When the relative humidity decreases from ambient to 10%, the average mass loss of these samples is about 5% (region I). However, in region III (RH > 70%) PVA-EG complexes become more hygroscopic than the PVA. Indeed, the curves corresponding to these complexes are well above than that of pure PVA. Thus, the hygroscopicity of these samples increases with the EG content in the complex. Between the ambient relative humidity and RH = 100%, the evolution of the mass of PVA-EG(50 wt%) complex represents about 80% of its initial mass. Under the same conditions of hydration, the mass of PVA changes only by 32%. For the others two binary complexes, PVA-EG(10 wt%) and PVA-EG(30 wt%), the hydration rate is about 40 and 62% respectively. In addition, we notice that the complexes containing > 50 wt% of EG present a very gluing aspect at high relative humidity.

The association of a low amount of H_3PO_4 with the PVA-EG complexes could leads to the formation of complexes that provide both interesting electrical and mechanical properties. The ternary complex PVA-EG-H_3PO_4 (Fig. 3e) presents a hygrometric behaviour similar to that of the PVA-EG complexes with an increase in mass from approximately 104% of its initial mass at RH = 100%. However, this complex preserves its mechanical properties and could be used as solid protonic electrolyte even at RH = 100%.

3.4. Influence of relative humidity on the ionic conductivity

Fig. 4 shows the effect of the surrounding relative humidity on the ionic conductivity of binary complexes: PVA-EG at different plasticizer contents and PVA-H_3PO_4(5 wt%) and the ternary complex PVA-EG(45 wt%)-H_3PO_4(5 wt%). In this figure we represent the effect of both the amount of the plasticizer in the complex and the rate of hydration on the ionic conductivity of these materials. The ionic

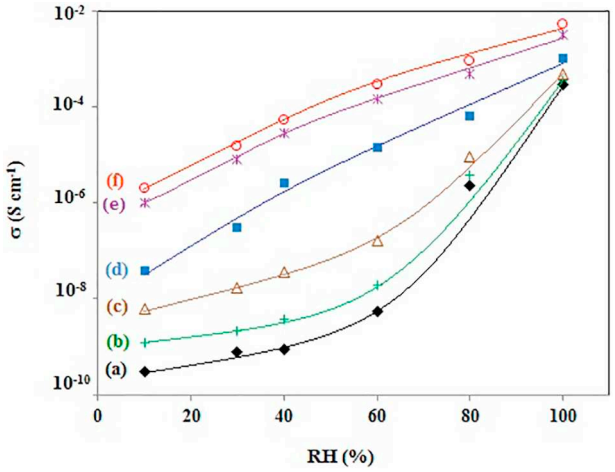

Fig. 4. Evolution of ionic conductivity as a function of RH of samples: (a) PVA, (b) PVA-EG(10 wt%), (c) PVA-EG(30 wt%), (d) PVA-EG(50 wt%), (e) PVA-H_3PO_4(5 wt%) and (f) PVA-EG(45 wt%)-H_3PO_4(5 wt%).

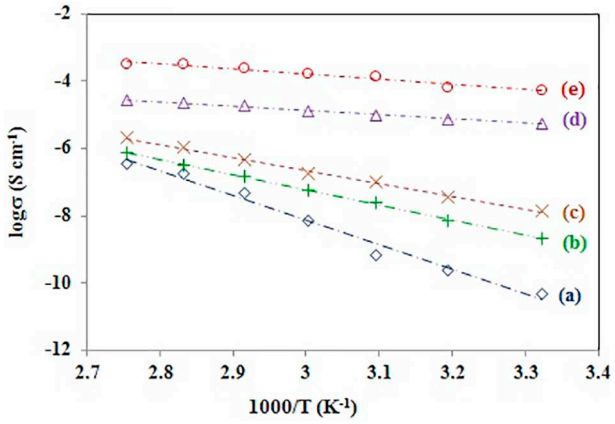

Fig. 5. Evolution of log(σ) as a function of the inverse of the temperature at RH = 40%: (a) PVA, (b) PVA-EG(10 wt%), (c) PVA-EG(30 wt%), (d) PVA-EG(50 wt%) and (e) PVA-EG(45 wt%)-H_3PO_4(5 wt%).

conductivity of all studied complexes increases with the increasing of the rate of ethylene glycol in the complex and also with the surrounding relative humidity. Indeed, the protonic conductivity of PVA increases from 3.0 10^{-10} S cm^{-1} at 10% RH to 3.0 10^{-4} S cm^{-1} at 100% RH, this corresponds to an improvement in the ionic conductivity by a factor of 10^6 [28]. However, PVA-EG complex containing 50 wt% of EG (Fig. 4d) presents electrical properties better than those of the PVA, its ionic conductivity increases from 3.9 10^{-8} S cm^{-1} to 9.9 10^{-4} S cm^{-1} when RH varies from 10 to 100% this corresponds to an increase in the ionic conductivity by a factor of 2.5 10^4. At low relative humidity (10%), PVA-EG(50 wt%) complex is about 130 times more conductor than the PVA, whereas at high RH (100%), the conductivity of the PVA-EG(50 wt%) complex is only three times more important than that of the PVA. Thus, the two binary complexes PVA-EG(10 wt%) (Fig. 4b) and PVA-EG(30 wt%) (Fig. 4c) have intermediate ionic conductivity between those of the PVA and PVA-EG(50 wt%) complexes. This can be explained by the fact that the presence of plasticizer in the complex increases the electrical mobility of protons (H^+) [16,51]. On the other hand, the water content in the complex, which depends on the relative humidity RH, affects simultaneously the concentration of the charge carriers and their electrical mobility. Thus, the plasticizer effect is more pronounced at low relative humidities. On the other hand, at high RH the effect of hydration water molecules shows a leveling effect of the plasticizer since their amount is sufficient to compete with the plasticizer.

Although the ionic conductivity of the PVA-EG binary complexes is better than that of the pure PVA over the entire interval of relative humidity, the electrical properties of these complexes are not sufficient to use as solid proton conducting electrolyte for electrochemical cells. To improve this ionic conductivity, the association of PVA and EG to a mineral acid, at low concentration, will be of great interest. These new complexes should have adequate electrical and mechanical properties for their application in cells.

Indeed, the ternary PVA-EG-H_3PO_4 complexes seem to be an excellent combination to obtain a relatively high protonic conductivity with suitable mechanical and hygroscopic properties. Moreover, these complexes may be less corrosive overlooked the active material of negative electrode if their acid content remains relatively low. The conductivity of the PVA- H_3PO_4(5 wt%) binary complex (3.1 10^{-3} S cm^{-1} at RH = 100%) is intermediate (Fig. 4e) between those of PVA-EG(50 wt%) and PVA-EG(45 wt%)-H_3PO_4(5 wt%) complexes. It is three times greater than that of the PVA-EG(50 wt%) complex. However, the ternary complex PVA-EG(45 wt%)-H_3PO_4(5 wt%) presents a protonic conductivity, at room temperature, equal to 5.2 10^{-3} S cm^{-1} at RH = 100% (Fig. 4f). This represents a protonic conductivity respectively 17, 5 and 1.7 times better than those of PVA, PVA-EG(50 wt%) and PVA-H_3PO_4(5 wt%) complexes. Therefore, this complex will be used as an electrolyte for "all-solid" Zn/MnO_2 cells.

3.5. Temperature dependence of conductivity

According to X-ray diffraction results, each studied PVA-based complex presents an amorphous structure at room temperature. This result constitutes an advantage for the use of this type of materials as ion conducting because, it is known that the contribution of amorphous phases in ionic conduction mechanism is determining [52].

The measurement of ionic conductivity over a wide range of temperature is a good indicator of the thermal stability of the solid polymer electrolytes. Fig. 5 shows the temperature-dependent conductivity of different PVA-based complexes at different temperature. From the plot, it is evident that as the temperature increases the ionic conductivity also increases for all these complexes. The increase in the conductivity with temperature may be due to the increased mobility of the charge carriers. Thus, these complexes exhibit an Arrhenius-type temperature dependence of the protonic conductivity, suggesting thermally activated proton conduction. The activation energy, which is the minimum energy required for proton transport, is obtained for each complex from the slope of Arrhenius plots using the following equation:

$$\sigma = \sigma_0 \, exp\left(\frac{-E_a}{RT}\right)$$

where σ is the proton conductivity in S cm^{-1}, σ_0 the pre-exponential factor function of temperature in the general case, E_a the activation energy (in kJ mol^{-1}), R the universal gas constant (= 8.314 J mol^{-1} K^{-1}) and T the absolute temperature (K).

The increasing in ionic conductivity of PVA-based complexes with temperature can be explained by the free volume model. As the temperature increases, the polymer electrolyte can expand easily and produce free volume [53]. Therefore, ions or polymer segments can move into the free volume causing its increase [6]. This improves the mobility of ions and segments of the polymer which enhance the conductivity.

On the other hand, to demonstrate the combined effect of the temperature and the hydration on the protonic conductivity of the prepared PVA-based complexes, we have studied the evolution of the protonic conductivity of different complexes, between 30 and 90 °C, at different RH. The values of the activation energy of these complexes are summarized in Table 1. Our results are similar to those reported in the literature for PVA-based complexes [11,16,19,44,54–56].

The results of Table 1 show a decrease in the activation energy of the studied complexes with RH. This proves the plasticizing effect of the

Table 1
Values of the activation energy in kJ mol^{-1} for the studied complexes.

	RH (%)			
	40	60	80	100
Compound	E_a (kJ mol^{-1})			
PVA	105	97.7	45.0	40.8
PVA-EG(10 wt%)	66.0	52.4	32.7	30.2
PVA-EG(30 wt%)	43.6	36.0	33.4	28.9
PVA-EG(50 wt%)	21.0	20.5	20.0	18.6
PVA-H_3PO_4(1 wt%)	93.0	68.9	54.0	35.6
PVA-EG(49 wt%)-H_3PO_4(1 wt%)	20.8	19.8	18.2	15.1
PVA-EG(45 wt%)- H_3PO_4(5 wt%)	20.4	18.5	13.4	9.0

hydration water in agreement with literature [28,57,58]. Thus, the PVA-EG(45 wt%)-H_3PO_4(5 wt%) complex presents the highest protonic conductivity and the lowest activation energy. This makes him a good electrolyte material for cells in these hydration conditions.

3.6. Electrochemical study

Ternary complex PVA-PWA(40 wt%)-H_3PO_4(40 wt%) combines both excellent electrical properties (1.8 10^{-2} S cm^{-1} at RH = 100%) with appreciable mechanical ones over a wide range of RH, its application as an electrolyte of "all-solid" Zn/MnO_2 system with cells of acceptable performances (70 Ah kg^{-1} and 120 Wh kg^{-1}) is possible. In our previous work [28], we showed that complexes with high concentration of H_3PO_4 cause corrosion of the negative electrode and consequently limit the performance of the cell. To overcome this problem, a complex containing a plasticizer (EG) with low amount of acid (PVA-EG(45 wt%)-H_3PO_4(5 wt%)) has been studied. This complex showed mechanical and electrical properties (5.2 10^{-3} S cm^{-1}, 9 kJ mol^{-1} at RH = 100%) adequate to its use in the "all-solid" cells.

3.6.1. Negative active mass composition

In this part, the positive electrode of these cells consists, referring to the literature works [34], of a mixture of MnO_2 and carbon black (5 wt %). The cathodic active mass is used in excess so that the cell capacity is limited by that of the negative electrode.

In a previous work, Telli and al. [32] have optimized the composition of the negative active mass of a Zn/MnO_2 cell. This study showed that the optimal composition, that led to a maximum capacity and specific energy at RH = 100% and at low discharge rate, corresponds to a mixture containing 65 wt% of zinc and 35 wt% of a hydrated zinc salt (AZS). This optimal composition was observed for this mixture exhibiting nearly equal grains surface areas of both constituents. Nevertheless, the electrochemical study shows that the negative electrode impedance is relatively important which probably limits its performances. In fact, the total impedance of the anode deduced from the intersection with the real axis (Fig. 6a) is about 2 kΩ. The value of this total impedance limits, particularly, the discharge rates of these cells. Therefore, an additional study, aiming the reduction of the impedance of the negative electrode, appears to be necessary. In this study, a low amount of AZS ($\leq$5 wt%) has been substituted by an equivalent amount of carbon black.

Fig. 6a shows a typical impedance diagram of Zn-based composite electrode recorded, at RH = 80%, just after the preparation of the cell: Zn-AZS(35 wt%)/MnO_2-CB(2 wt%). The first loop, that appears on the Nyquist diagram at high frequencies, is likely due to the ionic transport phenomenon in the electrolyte bulk. However, another capacitive loop, slightly flattened, appears in medium and low frequencies translating phenomena occurring at the negative electrode/electrolyte interface. Allowing for the form of this loop, these phenomena are multiples or it is a complex phenomenon. One of these capacitive loops presumably corresponds to a charge transfer resistance in parallel with a capacity of

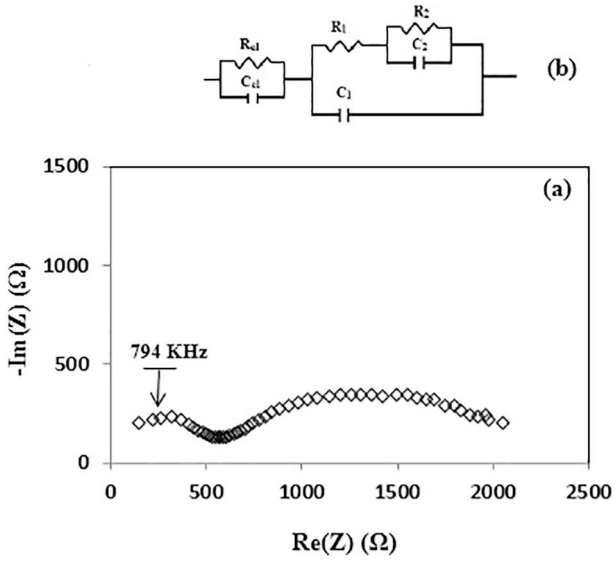

Fig. 6. a) Impedance diagram of the composite anode Zn-AZS(35 wt%) at RH = 80% and b) the equivalent electrical circuit with $R_{el}C_{el}$ the part relating to the impedance of the solid electrolyte.

the double layer. Considering the presence of metallic Zn in the anode and working conditions (often high relative humidity, presence of hydrated H^+ ions in the electrolyte), the other loop is probably due to the presence of a layer of zinc oxide (ZnO) formed at the solid electrolyte/anode interface. Indeed, the hydrated protons of the solid electrolyte can be reduced causing corrosion of the zinc surface in contact with the electrolyte. This behaviour has been reported in the literature [59–62] under comparable conditions. Thus, in the frequency domain explored, an equivalent electrical circuit can be proposed (Fig. 6b).

In order to identify the half-circle which corresponds to the charge transfer, we investigated by electrochemical impedance spectroscopy the behaviour of the negative electrode around the equilibrium using the linear approximation of the Butler-Volmer relationship. Impedance diagrams of the Zn-based composite electrode have been recorded, in the stationary state, using sinusoidal signal superimposed to continuous signal corresponding to the overvoltages between 0 and 20 mV with an increment of 5 mV. The representation of the evolution of $R_{tc}I$ (R_{tc} represents the charge transfer resistance and I the stationary current) as function of the overvoltage (η) must give a straight line which passes through the origin and of a slope equal to one.

The evolution of R_2I as a function of η (Fig. 7) is a straight line that passes through the origin and of a slope of 1.008. This proves that the

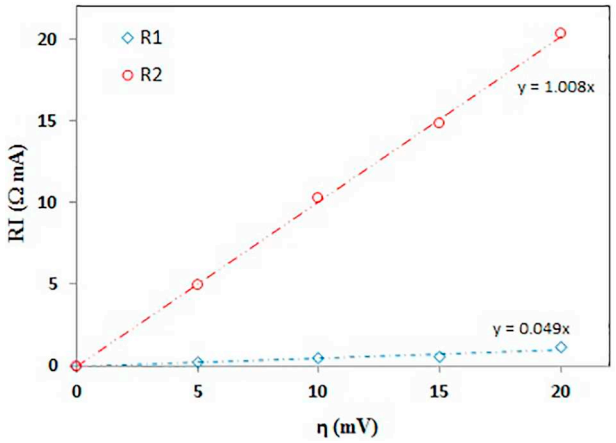

Fig. 7. Evolution of RI as function of the overvoltage applied to the electrode of zinc in contact with the PVA-based electrolyte.

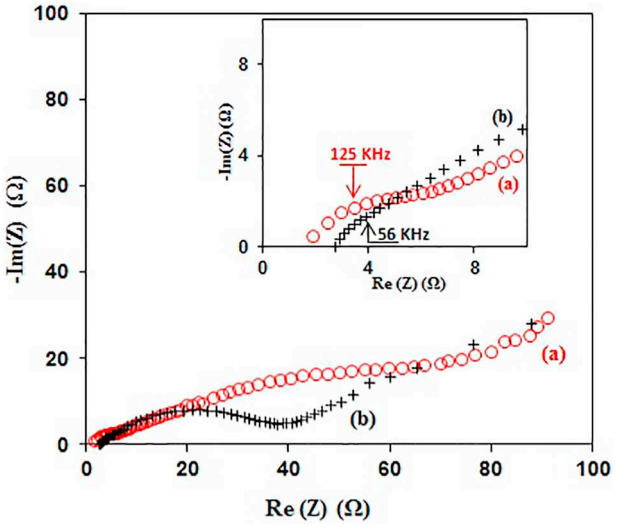

Fig. 8. Impedance diagram of a) pure zinc anode and b) the composite electrode Zn- AZS(33 wt%)-CB(2 wt%) at RH = 80%.

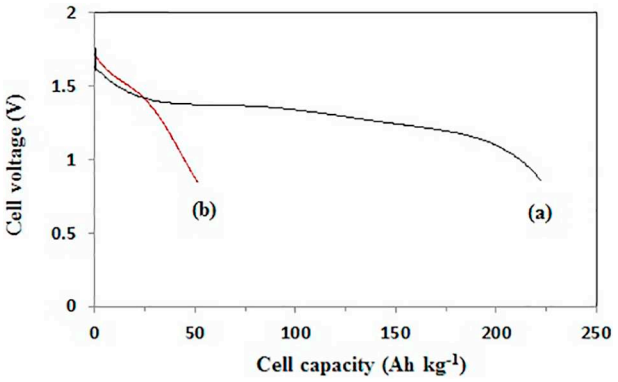

Fig. 9. Evolution of cell voltage of: (a) Zn-AZS(35 wt%)-CB(2 wt%)/PVA-EG(45 wt%)-H_3PO_4(5 wt%)/MnO_2-CB(5 wt%) and (b) Zn/PVA-PWA(40 wt%)-H_3PO_4(40 wt%)/MnO_2 [28] at regime discharge of 0.1 mA cm^{-2} and RH = 100%.

last capacitive loop of the impedance diagram (appears at low frequencies) is due to a charge transfer resistance, of the anodic reaction: $Zn \leftrightarrows Zn^{2+} + 2e^-$, coupled to a capacity of the double layer. However, the other loop (appears at medium frequencies) of resistance R_1 gives a straight line of a slope of 0.049, clearly less than 1, corresponds to the formation of a ZnO layer.

Fig. 8b shows an impedance diagram of the composite electrode: Zn-AZS(33 wt%)-CB(2 wt%) recorded at RH = 80%. The global impedance of this composite electrode is of the order of a decade of ohms. This represents a reduction of the total impedance by a factor of ~ 40 times compared to that of the Zn-AZS(35 wt%) composite electrode and about 2 times compared to that of the pure Zn electrode. This shows the positive effect of carbon black on the reduction of the value of the impedance of composite electrode. The Zn-AZS(34 wt%)-CB(1 wt%) composite electrode global impedance has an intermediate value between those of the pure zinc electrodes and Zn-AZS(33 wt%)-CB(2 wt%). On the other hand, the presence of a relatively high amount (5 wt%) of carbon black in the composite electrode influences negatively on the mechanical properties of the pellets formed. Indeed, the pellets thus obtained are breakable and carry cracks. Considering these results, the optimal composition of the negative electrode is: 65 wt% of Zn, 33 wt% of AZS and 2 wt% of carbon black. Thus, this composite electrode: Zn-AZS(33 wt%)-CB(2 wt%) will be used as the negative electrode during the discharge of Zn/MnO_2 cell. It seems that it permits to have cells with better performances. Indeed, it presents a relatively low impedance and it contains a sufficient amount of AZS which confers it a high specifics capacity and energy.

3.6.2. Performance of Zn/MnO_2 cell

Fig. 9 shows a typical discharge curve recorded on a two electrodes cell: Zn-AZS(33 wt%)-CB(2 wt%)/PVA-EG(45 wt%)-H_3PO_4(5 wt%)/MnO_2-CB(5 wt%), compared to that of the non-optimized cell: Zn/PVA-PWA(40 wt%)-H_3PO_4(40 wt%)/MnO_2 [28]. This discharge was carried out at a constant current density of 0.1 mA cm^{-2} with lower cut-off voltage of 0.9 V. The open circuit voltage (OCV) value for the non-optimized cell (Fig. 9b) is close to 1.9 V and the ionic conductivity of PVA-PWA(40 wt%)-H_3PO_4(40 wt%) electrolyte is 1.8 10^{-2} S cm^{-1} at RH = 100% [28]. In the other hand, the open-circuit voltage for the optimized cell (Fig. 9a) has reached a high value of 1.8 V. When the cell delivers a current, the cell voltage decreases due to the ohmic drop. Then, a pseudo-plateau, around 1.4 V, is established along the major part of the discharge; its shape is characteristic of cells based on MnO_2. This cell provides an experimental specific capacity and an energy, reported to the unit of the negative active mass exceeding 222 Ah kg^{-1} and 286 Wh kg^{-1}, respectively. These performances are significantly higher than those reported in the literature [28,32,34,63,64] for comparable systems. This shows the very positive effect of the various additives used in the electrolyte and the negative electrode on the electrical performances of the studied Zn/MnO_2 cell.

4. Conclusion

Complexes containing PVA, EG and H_3PO_4 were prepared and characterized by different techniques namely: XRD, FTIR and EIS. The conductivity of the studied PVA-based binary complexes varies as a function of the level of the plasticizer and of the hydration water content. Indeed, the association of the ethylene glycol to the PVA permits to improve its protonic conductivity by a factor of 130 times at low relative humidity and by a factor of 3 times at very high humidities. In spite of this improvement, the value of the proton conductivity (9.9 10^{-4} S cm^{-1} at RH = 100%) is not sufficient for a possible use of these PVA-EG binary complexes as solid electrolyte of batteries. However, the combination of a mineral acid, in low quantity, with the PVA-EG complex gives films with appropriate electrical and mechanical properties for applications in “all-solid” cells. Thus, the ternary complex: PVA-EG(45 wt%)-H_3PO_4(5 wt%) presents a maximum proton conductivity of 5.2 10^{-3} S cm^{-1} at RH = 100% and at room temperature with an activation energy of 9 kJ mol^{-1}.

On the other hand, this new complex has been used as proton conducting electrolyte in “all-solid” Zn/MnO_2 cell. The composition of the anodic active mass has been optimized in order to have a low impedance of the negative electrode while maintaining an important specific capacity and energy. This has been achieved by a substitution of 2 wt% of the hydrated salt associated to Zn in the negative electrode by an equivalent amount of carbon black. The association of the negative electrode and the electrolyte, of optimal compositions, to a MnO_2-based positive electrode gives a cell with very appreciable performances. Indeed, a capacity of 220 Ah kg^{-1} and a specific energy of 286 Wh kg^{-1} values were reached. The optimization of the composition of the positive electrode could be of great interest in the improvement of the performances of this cell.

References

[1] S. Chandra (Ed.), Superionic Solids-Principles and Application, North Holland, Amesterdam, 1981.
[2] M.Z.A. Munshi (Ed.), Handbook of Solid-State Batteries and Capacitors, World Scientific, Singapore, 1995.
[3] B. Scrosati, R.J. Neat, Lithium-polymer batteries, in: B. Scrosati (Ed.), Applications of Electroactive Polymers, Chapman & Hall, London, 1993, p. 182.
[4] N. Lakshmi, S. Chandra, J. Power Sources 108 (2002) 256–260.

[5] M.B. Armand, Ann. Rev. Mater. Sci. 16 (1986) 245–261.
[6] M.A. Ratner, D.F. Shriver, Chem. Rev. 88 (1988) 109–124.
[7] B. Scrosati, Philos. Mag. B 59 (1989) 151–160.
[8] C.W. Walker Jr., Mark Salomon, J. Electrochem. Soc. 140 (1993) 3409–3412.
[9] A. Awadhia, S.L. Agrawal, Solid State Ionics 178 (2007) 951–958.
[10] G.K. Prajapati, P.N. Gupta, Nucl. Instrum. Methods Phys. Res. B 267 (2009) 3328–3332.
[11] H. Gao, Q. Tian, K. Lian, Solid State Ionics 181 (2010) 874–876.
[12] A. Lewandowski, K. Skorupska, J. Malinska, Solid State Ionics 133 (2000) 265–271.
[13] G.M. Wu, S.J. Lin, C.C. Yang, J. Membr. Sci. 280 (2006) 802–808.
[14] S. Sang, J. Zhang, Q. Wu, Y. Liao, Electrochim. Acta 52 (2007) 7315–7321.
[15] S. Sang, Q. Wu, Z. Gan, Electrochim. Acta 53 (2008) 5065–5070.
[16] G.K. Prajapati, R. Roshan, P.N. Gupta, J. Phys. Chem. Solids 71 (2010) 1717–1723.
[17] R.A. Vargas, V.H. Zapata, E. Matallana, M.A. Vargas, Electrochim. Acta 46 (2001) 1699–1702.
[18] B. Chatterjee, P.N. Gupta, J. Non-Cryst. Solids 358 (2012) 3355–3364.
[19] F. Ahmad, E. Sheha, J. Adv. Res. 4 (2013) 155–161.
[20] H. Gao, K. Lian, Electrochim. Acta 56 (2010) 122–127.
[21] L. Li, L. Xu, Y. Wang, Mater. Lett. 57 (2003) 1406–1410.
[22] K. Hatakeyama, H. Sakaguchi, K. Ogawa, H. Inoue, C. Iwakura, T. Esaka, J. Power Sources 124 (2003) 559–563.
[23] Y. Cui, J. Mao, Q. Wu, Mat. Chem. Phys. 85 (2004) 416–419.
[24] U.B. Mioc, M.R. Todorovic, Ph. Colomban, I. Holclajtner-Antunovic, Solid State Ionics 176 (2005) 3005–3017.
[25] W.E. Mahmoud, A.A. Al- Ghamdi, M.W. Kadi, Radiat. Phys. Chem. 81 (2012) 693–696.
[26] U. Thanganathan, R. Bobba, J. Alloys Compd. 540 (2012) 184–191.
[27] H. Gao, H. Wu, K. Lian, Electrochem. Commun. 17 (2012) 48–51.
[28] Z. Gharnout, L. Telli, A. Merrouche, S. Walter, A. Hadj Mebarek, Solid State Ionics 256 (2014) 68–75.
[29] M. Higa, M. Sugita, S. Maesowa, N. Endo, Electrochim. Acta 55 (2010) 1445–1449.
[30] C.C. Yang, S.-J. Chiu, C.-T. Lin, J. Power Sources 177 (2008) 40–49.
[31] A.K. Sahu, G. Selvarani, S.D. Bhat, S. Pitchumani, P. Sridhar, A.K. Shukla, N. Narayanan, A. Banerjee, N. Chandrakumar, J. Membr. Sci. 319 (2008) 298–305.
[32] L. Telli, A. Hammouche, B. Brahimi, R.W. De Doncker, J. Power Sources 103 (2002) 201–206.
[33] A. Hammouche, J.P. Caire, N. Chelali, M. Boutahala, Electrochim. Acta 42 (1997) 2511–2515.
[34] M.F.Z. Kadir, S.R. Majid, A.K. Arof, Electrochim. Acta 55 (2010) 1475–1482.
[35] C.C. Yang, G.M. Wu, Mater. Chem. Phys. 114 (2009) 948–955.
[36] S.K. Shahenoor Basha, G. Sunita Sundari, K. Vijaya Kumar, Mater. Today: Proc. 3 (2016) 11–20.
[37] G.K. Prajapati, P.N. Gupta, Physica B 406 (2011) 3108–3113.
[38] W. Wu, H. Tian, A. Xiang, J. Polym. Environ. 20 (2012) 63–69.
[39] P.D. Hong, J.-H. Chen, H.-L. Wu, J. Appl. Polym. Sci. 69 (1998) 2477–2486.
[40] C.W. Lin, R. Thangamuthu, C.J. Yang, J. Membr. Sci. 253 (2005) 23–31.
[41] S.A.M. Zobir, Z. Zainal, M.Z. Hussein, Mat. Chem. Phys. 124 (2010) 477–481.
[42] J. Wu, M.J. Wang, J.P.W. Stark, J. Quant. Spectrosc. Radiat. Transf. 102 (2006) 228–235.
[43] M. Stefanescu, M. Stoia, O. Stefanescu, C. Davidescu, G. Vlase, P. Sfirloaga, Rev. Roum. Chim. 55 (2010) 17–23.
[44] Q. Tang, K. Huang, G. Qian, B.C. Benicewicz, J. Power Sources 229 (2013) 36–41.
[45] Y. Liu, Y. Zhang, G. Ma, Z. Wang, K. Liu, H. Liu, Electrochim. Acta 88 (2013) 519–525.
[46] L.M. Ai, W. Feng, J. Chen, Y. Liu, W. Cai, Mater. Chem. Phys. 109 (2008) 131–136.
[47] H.L. Lin, S.H. Wang, C.K. Chiu, T.L. Yu, L.C. Chen, C.C. Huang, T.H. Cheng, J.M. Lin, J. Membr. Sci. 365 (2010) 114–122.
[48] Z. Yue, J. Economy, C.L. Mangun, Carbon 41 (2003) 1809–1817.
[49] J.R. Dyer, Applications of Absorption Spectroscopy of Organic Compounds, Prentice-Hall of India, New Delhi, 1991, p. 31.
[50] P.N. Gupta, K.P. Singh, Solid State Ionics 86-88 (1996) 319–323.
[51] P.N. Gupta, Indian. J. Pure & Appl. Phys. 46 (2008) 657–659.
[52] C. Berthier, W. Gorecki, M. Minier, M. Armand, J.M. Chabagno, P. Riguaud, Solid State Ionics 11 (1983) 91–95.
[53] A.R. Polu, R. Kumar, K.V. Kumar, Adv. Mat. Lett. 3 (2012) 406–409.
[54] U. Thanganathan, D. Dixon, S.L. Ghatty, B. Rambabu, Int. J. Hydrog. Energy 37 (2012) 17180–17190.
[55] C.C. Yang, S.J. Lue, J.Y. Shih, J. Power Sources 196 (2011) 4458–4467.
[56] M. Erkartal, H. Usta, M. Citir, U. Sen, J. Membr. Sci. 499 (2016) 156–163.
[57] X. Tang, S. Alavi, Carbohydr. Polym. 85 (2011) 7–16.
[58] X. Jiang, T. Jiang, L. Gan, X. Zhang, H. Dai, X. Zhang, Carbohydr. Polym. 90 (2012) 1677–1684.
[59] R.K. Ghavami, Z. Rafiei, S.M. Tabatabaei, J. Power Sources 164 (2007) 934–946.
[60] M. Minakshi, M. Ionescu, Int. J. Hydrogen Energy 35 (2010) 7618–7622.
[61] G.Q. Zhang, X.G. Zhang, Solid State Ionics 160 (2003) 155–159.
[62] D. Qu, Electrochem. Commun. 8 (2006) 1527–1530.
[63] C. Justin Raj, K.B.R. Varma, Electrochim. Acta 56 (2010) 649–656.
[64] L. Telli, A. Merrouche, A. Ghanem, S. Walter, A. Hadj Mebarek, Solid State Ionics 181 (2010) 701–704.